Guiding Polymers to Perfection: Macroscopic Alignment of Nanoscale Domains

Deepak Sundrani,[†] S. B. Darling,[‡] and S. J. Sibener*,[†]

The James Franck Institute and the Department of Chemistry, The University of Chicago, 5640 South Ellis Avenue, Chicago, Illinois 60637, and Materials Science Division, Argonne National Laboratory, 9700 S. Cass Avenue, Argonne, Illinois 60439

ABSTRACT

Nanoscale diblock copolymer domains are aligned via top-down/bottom-up hierarchical assembly. Grating substrates template cylinder alignment with demonstrated 5000:1 aspect ratio for 100 μm domains extendable to arbitrary length scales. Depending on trough depth and amount of deposited polymer, aligned domains are (1) confined to the channels or (2) expanded across the grating frequently with (3) a complete absence of defects. This methodology can be exploited in hybrid hard/soft matter systems for electronics, catalysis, and sensors.

Fabrication of macroscopic domains of periodic nanoscale structures using self-organizing systems has garnered significant attention because of the simplicity and low cost of the method.[1] Ultrathin diblock copolymer films, in particular, are promising candidates for bottom-up nanotemplates in hybrid organic−inorganic electronic,[2] optical, and magnetic[3−5] devices. These systems self-assemble into microphase separated domains with a length scale tunable through the heart of the nanoscale (10−100 nm); however, without further constraint, the domains have no preferred orientation and form a disordered "fingerprint" structure.[6,7] Localized alignment of cylindrical domains has been reported using solvent prewetting,[8] electric fields,[9] directional crystallization,[10] and other schemes. These approaches, though, tend to produce either only short-range order or random domain orientation. In this paper, we present a new general method for defining an orientation and eliminating defects via the introduction of geometric substrate anisotropy.[11] Graphoepitaxy[12−14] is applied to the cylindrical diblock copolymer phase to overcome the stubborn disorder intrinsic to this structure. Three novel results will be presented: (1) alignment of cylindrical polymer domains in confined volumes, (2) extension of this substrate-induced alignment above and beyond the confined volumes, and (3) virtually defect-free domains in contrast to results obtained using other cylinder alignment techniques. Alignment is achieved using lithographically assisted self-assembly—a combined top-down/bottom-up methodology.

Diblock copolymer composed of polystyrene and polyisoprene, denoted PS-*b*-PI, with a molecular weight of 22 000 g/mol and a polydispersity of 1.08, was modified to polystyrene-*block*-poly(ethylene-*alt*-propylene) (PS-*b*-PEP) by selective hydrogenation of the polyisoprene block.[15] PS-*b*-PEP has 27 wt % PS so that, in the bulk, the copolymer forms hexagonally packed PS cylinders in the PEP matrix. The spacing between the cylinders is 26.6 nm and the natural thickness of one layer of cylinders, L, equals 23 nm as determined by a calibrated AFM measurement. Thin films of this diblock copolymer were spin-cast (at 5000 rpm) from 1.55% toluene solutions onto flat and topographically patterned silicon nitride substrates. These substrates, containing varied square wave grating patterns, were prepared in a silicon nitride layer by electron beam lithography using a Hitachi S-2700 scanning electron microscope (SEM) and reactive ion etching (Figure 1b). These films consist of cylindrical microdomains of PS embedded in a PEP matrix when annealed (115−135 °C) above the glass transition temperature under an argon atmosphere. Each grating contained troughs of different widths ranging from 200 nm to 1.5 μm in increments of 100 nm; the trough length was always 100 μm. Crest widths were a constant ∼750 nm. Gratings of two different depths, 35 and 95 nm, were used for these experiments. These depths were selected to comfortably accommodate one layer and three layers of cylinders, respectively.

Before discussing the behavior of PS-*b*-PEP thin films on patterned substrates, it is useful to review their behavior on a typical flat silicon nitride substrate. PS prefers to wet the silicon nitride/polymer interface whereas PEP exhibits an

* Corresponding author. E-mail: s-sibener@uchicago.edu.
† The University of Chicago
‡ Argonne National Laboratory.

Report Documentation Page

1. REPORT DATE **08 DEC 2003**	2. REPORT TYPE	3. DATES COVERED **00-00-2003 to 00-00-2003**

4. TITLE AND SUBTITLE	5a. CONTRACT NUMBER
Guiding Polymers to Perfection: Macroscopic Alignment of Nanoscale Domains	5b. GRANT NUMBER
	5c. PROGRAM ELEMENT NUMBER
6. AUTHOR(S)	5d. PROJECT NUMBER
	5e. TASK NUMBER
	5f. WORK UNIT NUMBER

7. PERFORMING ORGANIZATION NAME(S) AND ADDRESS(ES) **University of Chicago,James Franck Institute ,Department of Chemistry,Chicago,IL,60637**	8. PERFORMING ORGANIZATION REPORT NUMBER

9. SPONSORING/MONITORING AGENCY NAME(S) AND ADDRESS(ES)	10. SPONSOR/MONITOR'S ACRONYM(S)
	11. SPONSOR/MONITOR'S REPORT NUMBER(S)

12. DISTRIBUTION/AVAILABILITY STATEMENT
Approved for public release; distribution unlimited

13. SUPPLEMENTARY NOTES

14. ABSTRACT
see report

15. SUBJECT TERMS

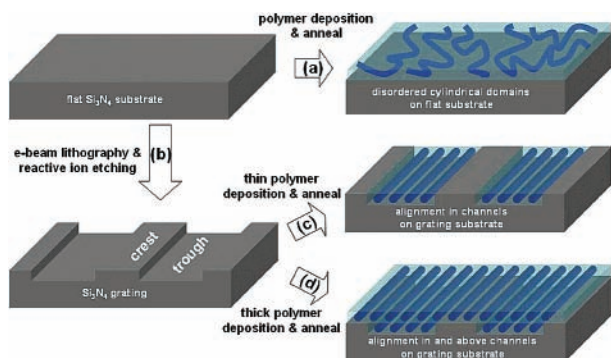| 16. SECURITY CLASSIFICATION OF:			17. LIMITATION OF ABSTRACT	18. NUMBER OF PAGES	19a. NAME OF RESPONSIBLE PERSON
a. REPORT **unclassified**	b. ABSTRACT **unclassified**	c. THIS PAGE **unclassified**	**Same as Report (SAR)**	**4**	

Figure 1. Schematic illustration of the strategy used to fabricate parallel arrays of aligned diblock copolymer cylindrical domains. (a) A thin film of diblock copolymer spin-coated and annealed on a flat substrate forms disordered cylindrical domains. (b) Grating patterns were prepared on a flat Si_3N_4 substrate by e-beam lithography and reactive ion etching. (c) A lower coverage of polymer on a patterned substrate, after annealing, forms aligned cylindrical domains parallel to the trough edges in the confined volumes of the troughs. (d) For a higher coverage of polymer, alignment in the troughs induces alignment above and beyond the confined volumes of the troughs.
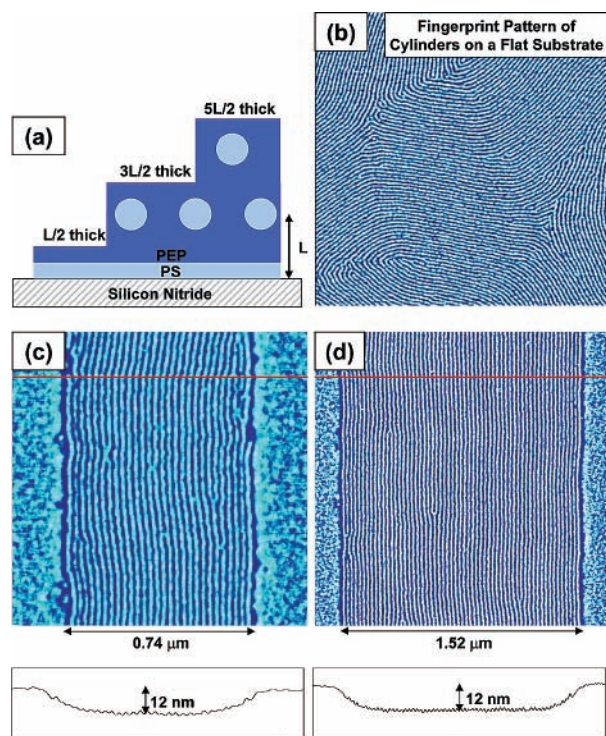

Figure 2. Influence of spatial confinement. (a) Schematic of diblock copolymer film on Si_3N_4 substrate. (b) Phase AFM image, $2 \, \mu m \times 2 \, \mu m$, showing typical disordered fingerprint pattern of an annealed film on a flat substrate. On a substrate with 35 nm deep channels, annealing aligns the cylinders across the entire trough width and along the full 100 μm length. (c) 1.1 $\mu m \times 1.1 \, \mu m$, and (d) 1.9 $\mu m \times 1.9 \, \mu m$ show phase AFM images of two such troughs. Height profiles show corrugation of 12 nm from the crests to the troughs.

affinity for the polymer/air interface (Figure 2a). The quantized film thickness due to asymmetric wetting of this diblock copolymer corresponds to odd multiples of $L/2$, that is, $(2n+1)L/2$, where n is an integer and L is 23 nm. For $L/2$ thickness, a monolayer of diblock copolymer covers the

substrate which, due to the absence of cylinders, appears featureless when imaged using tapping mode atomic force microscopy (AFM). When the film is thicker than $L/2$ ($3L/2$, $5L/2$, etc.), the underlying cylinders of PS parallel to the film plane appear as a characteristic fingerprint pattern when imaged with tapping mode AFM (Nanoscope IIIa/IV, Digital Instruments Multimode SPM) under hard tapping conditions. The difference in contrast in the phase image (Figure 2b) is observed because of the difference in elastic modulus of the two diblock components. This thin film sample prepared on a flat substrate and annealed at 130 °C for 24 h does not have any preferential orientation of cylinders and contains a number of defects despite extensive annealing (Figure 1a).

In contrast to thin films on flat substrates, when a polymer film is prepared on a substrate patterned with 35 nm deep grating lines, the behavior of cylindrical domains is entirely different. For this sample only a monolayer of diblock copolymer ($L/2$ thick film) remains on the crests, whereas the troughs get completely filled with the polymer. Film thickness of ~35 nm in the troughs equals an approximately $3L/2$ thick film, i.e., a film with only one layer of cylinders. The preferential interaction of PS with the trough's sidewalls drives the alignment of cylindrical domains along the edges of the troughs.[16] Also, the presence of the brush layer along the trough sidewalls causes the first imaged polymer domain along the trough edges to appear wider (Figure 2c). Following brief annealing (2 h), one or two cylinders located along the edges are observed to align. When the sample is annealed for a longer duration (130 °C for 24 h), the aligned domains ripen, resulting in perfectly aligned cylindrical domains across the entire trough width. This edge-ripening process is analogous to zone-refining. The alignment is present along the full 100 μm length of all the troughs regardless of width (Figure 1c). Figure 2c and Figure 2d show this aligned structure for two such troughs of widths 0.74 μm and 1.52 μm, respectively. The section profiles in Figure 2 show that the film is flat in the troughs and the troughs are almost completely filled with the polymer; the corrugation of 12 nm from the crests to the troughs is attributable to the $L/2$ thick film present on the crests. It is interesting to observe that cylinders closely follow the geometry of the trough edges. When there is a significant deviation in trough width along its length due to lithographic imperfections, defects are created. We have observed that the polymer accommodates structurally similar defects reproducibly.

Alignment has also been routinely observed, surprisingly, to extend beyond the confined volumes of the etched channels. In Figure 3, this effect is seen for a region near the edge of a 95 nm deep grating that contains a film thicker than the channel depth. The topmost layer of cylinders of the $11L/2$ thick film in the troughs (T in Figure 3) is above the confined volumes of the troughs, but it is still aligned due to interactions with the underlying confined cylinders. This alignment, in turn, induces the lateral alignment of cylinders beyond the confined volumes of the troughs (Figure 1d), and we observe alignment of cylinders on the crests. Note that the bulk cylinder registry has not been explored, though further investigations to ascertain the stacking arrangement

Figure 3. Large-scale alignment of cylinders. Phase AFM image, 3.8 μm × 5.2 μm. This sample was prepared on a substrate with 95 nm deep troughs and annealed at 130 °C for 30 h. Alignment of underlying cylinders in the troughs not only induces alignment of cylinders above the troughs but it also aligns a single layer of cylinders on the crests. The troughs (T) have an $11L/2$ thick film, and the crests (C) have a $3L/2$ thick film. The trough marked T_1 has a $9L/2$ thick film and the crest marked C_1 has an $L/2$ thick film; therefore, this crest appears featureless.

are underway. For this coverage, the thickness of the film on the crests corresponds to one layer of cylinders (~35 nm). The few defects observed in this image are due to lithographic limitations. We expect that optimizing the procedure used to create the gratings would eliminate virtually all defects in the aligned regions. Even for films that are ~103 nm ($9L/2$) thick in the troughs (marked T_1 in Figure 3) on this 95 nm deep grating, we have observed that the alignment of cylindrical domains in underlying troughs induces alignment of cylinders both above the troughs and laterally onto the crests. Channels shallower than 35 nm do not support confined cylinder formation. It is our observation that any depth of the trough more than 35 nm, when over-filled, will lead to alignment beyond the confined volumes of the troughs. This methodology can presumably be utilized to align nanoscale polymer domains across an entire surface.

To ascertain the mechanism of alignment, we have observed the growth of cylinder alignment as a function of annealing time in troughs of ~280 nm width (95 nm deep) on a sample prepared using 1.55% polymer solution and a spinning speed of 5000 rpm. Here, the polymer film thickness in the troughs is ~103 nm ($9L/2$), whereas only ~12 nm ($L/2$) is present on the crests. Therefore, the surface of the crests is featureless. At lower annealing times (Figure 4a), at most two cylinders align along the trough edges, and many defects are present in the center of the troughs. Subsequent annealing leads to improvement in alignment with larger aligned cylindrical domains, but there are still perpendicularly oriented defects present as a vestige of the original flow direction[11] during annealing (Figure 4b). Further annealing removes even these defects, resulting in perfectly aligned cylindrical domains along the entire length of these narrow troughs (Figure 4c). The perfection in Figure 4c has been

Figure 4. Alignment mechanism. Sequential phase AFM images, 1 μm × 1 μm, of a film prepared on a 95 nm deep grating pattern and ~280 nm wide channels and annealed (a) at 115 °C for 2 h and then at 135 °C for (b) 6 h, and (c) 10 h. (d) Phase AFM image showing the cylinders following the curvature of an ~830 nm wide channel. Similar sequence for ~600 nm wide channels and annealing times of (e) 9 h, (f) 14 h, (g) 19 h, (h) 24 h, and (i) 33 h at 130 °C. Height profiles may exhibit some curvature near edges for incompletely filled channels.

seen to extend the full 100 μm length of the lithographic channels, suggesting that this phenomenon is unbounded in length. Therefore, this sequence of time-lapse images during the annealing process demonstrates the following mechanism: one or two cylinders initially align along the edges, then, at random locations along the troughs, this alignment ripens across the full width; the final stage of alignment is achieved by merging these smaller perfected regions.

We have also observed the evolution of domain alignment with annealing time for 95 nm deep and ~600 nm wide troughs. When the sample is annealed for 9 h (Figure 4e), one or two cylinders align along the edges of the troughs, but the cylinders in the center of the troughs are largely aligned across the troughs. This, again, is due to cylinders aligning along the initial direction of polymer flow during film preparation.[11] After 14 h of annealing, alignment parallel to the trough edges begins to grow at various spots along the length of the trough, so that there are regions of disordered cylinders present between the domains which have better alignment. The struggle of cylindrical domains to change their direction of orientation from perpendicular to parallel with respect to the trough edges causes the distortion of the cylinder spacing, as seen in Figure 4f. The domains with perfect alignment grow with further annealing to assimilate less perfect regions, and, at 33 h, the cylindrical domains are aligned along the entire length of the trough (Figure 4i). At this point, the spacing between the cylinders also equals its equilibrium value of 26.6 nm. Parallel flow along the channels cannot account for the observed alignment because there is no net flow along the length of the trough. The kinetics of this process varies with trough width, with wider troughs requiring additional annealing. Overall, we have observed the same growth mechanism for alignment in both narrow (~280 nm) and wide (~600 nm) troughs,

suggesting it is generally applicable to all relevant widths. For templating applications, curved or angled geometries would also be useful. We believe the guided alignment presented here is not restricted to straight architectures. The trough end depicted in Figure 4d illustrates the ability of the polymer cylinders to follow a curving channel without introducing any defects.

In summary, we have reported a simple method to align cylindrical domains in confined volumes initiated by the preferential wetting layer of PS on the vertical sidewalls of the troughs. Aligned domains templated by the lithographic channels are often defect-free over macroscopic length scales. The alignment occurs for single or multiple layers of cylinders, hence any trough depth greater than the film thickness for one layer of cylinders will produce alignment. Though not discussed in detail here, this vertical extension of the substrate-induced alignment makes possible the growth of three-dimensionally ordered nanoscale systems with high aspect ratios. For a higher coverage of polymer, alignment in the troughs induces not only alignment of cylinders above the troughs themselves but, through lateral propagation of order similar to zone-refining, it can also align cylinders on the crests. This approach allows for long-range order of cylinders over a large region with ramifications for the development of nanoscale templates and devices.[17] Note that the length scale of the lithographic patterning is at least an order of magnitude larger than the length scale present in the final polymer structure, and yet this nanoscale order extends to macroscopic scales. Furthermore, the flexibility of the copolymer enables it to smooth over defects created in the etching process. Pairing top-down and bottom-up techniques is a promising, and perhaps necessary, bridge between the parallel self-organization of molecules and the structural control of current technology.

References

(1) Park, M.; Harrison, C.; Chaikin, P. M.; Register, R. A.; Adamson, D. H. *Science* **1997**, *276*, 1401−1404.
(2) Thurn-Albrecht, T.; Schotter, J.; Kästle, G. A.; Emley, N.; Shibauchi, T.; Krusin-Elbaum, L.; Guarini, K.; Black, C. T.; Tuominen, M. T.; Russell, T. P. *Science* **2000**, *290*, 2126−2129.
(3) Asakawa, K.; Hiraoka, T.; Hieda, H.; Sakurai, M.; Kamata, Y.; Naito, K. *J. Photopolym. Sci. Technol.* **2002**, *15*, 465−470.
(4) Cheng, J. Y.; Ross, C. A.; Thomas, E. L.; Smith, H. I.; Lammertink, R. G. H.; Vancso, G. J. *IEEE Trans. Magn.* **2002**, *38*, 2541−2543.
(5) Bal, M.; Ursache, A.; Tuominen, M. T.; Goldbach, J. T.; Russell, T. P. *Appl. Phys. Lett.* **2002**, *81*, 3479−3481.
(6) Hahm, J.; Sibener, S. J. *J. Chem. Phys.* **2001**, *114*, 4730.
(7) Harrison, C.; Adamson, D. A.; Cheng, Z.; Sebastian, J. M.; Sethuraman, S.; Huse, D. A.; Register, R. A.; Chaikin, P. M. *Science* **2000**, *290*, 1558.
(8) Hahm, J.; Sibener, S. J. *Langmuir* **2000**, *16*, 4766−4769.
(9) Morkved, T. L.; Lu, M.; Urbas, A. M.; Ehrichs, E. E.; Jaeger, H. M.; Mansky, P.; Russell, T. P. *Science* **1996**, *273*, 931−933.
(10) Park, C.; De Rosa, C.; Thomas, E. L. *Macromolecules* **2001**, *34*, 2602−2606.
(11) Sundrani, D.; Sibener, S. J. *Macromolecules* **2002**, *35*, 8531−8539.
(12) Cheng, J. Y.; Ross, C. A.; Thomas, E. L.; Smith, H. I.; Vansco, G. J. *Appl. Phys. Lett.* **2002**, *81*, 3657−3659.
(13) Segalman, R. A.; Yokoyama, H.; Kramer, E. J. *Adv. Mater.* **2001**, *13*, 1152−1155.
(14) Segalman, R. A.; Hexemer, A.; Hayward, R. C.; Kramer, E. J. *Macromolecules* **2003**, *36*, 3272.
(15) Adams, J. L.; Quiram, D. J.; Graessley, W. W.; Register, R. A.; Marchand, G. R. *Macromolecules* **1998**, *31*, 201.
(16) Yokoyama, H.; Mates, T. E.; Kramer, E. J. *Macromolecules* **2000**, *33*, 1888.
(17) Lopes, W. A.; Jaeger, H. M. *Nature* **2001**, *414*, 735.

NL035005J